Magn Reson Med Sci
doi:10.2463/mrms.tn.2022-0053 Published Online: November 30, 2022

TECHNICAL NOTE

Using Phase Difference Information to Detect Errors in the Flip Angle Measured with Actual Flip Angle Imaging at 7T

Tsuyoshi Matsuda[1*], Yuji Iwadate[2], Futoshi Mori[1], Kota Takeda[1], and Makoto Sasaki[1]

Flip angle (FA) measurements using the actual flip angle imaging (AFI) method may induce significant errors in ultrahigh fields. We aimed to develop a method for detecting errors in FA measurements using phase information at 7 tesla. We performed computer simulations to elucidate the relationship between the FA calculation errors and the phase difference between the two AFI source images. We then examined whether a method based on the phase difference could detect FA calculation errors and determine the prescribed nominal FA of the scanner for accurate measurements in phantoms and healthy volunteers. The simulations confirmed that the calculated FA values erroneously decreased when the longitudinal magnetization and phase in one of the source images were inverted. Tests on phantoms and human subjects demonstrated that the phase difference information between the source images with a cut-off of 90° could readily detect FA calculation errors in the AFI method.

Keywords: *actual flip angle imaging, B1+ heterogeneity, flip angle measurement, phase difference, ultrahigh field magnetic resonance imaging*

Introduction

One of the issues in MRI at high magnetic fields is the non-uniform signal intensity of the images owing to the heterogeneity of the RF excitation field (B1+), which depends on the dielectric properties of the RF after penetrating the human body.[1,2] B1+ heterogeneity can cause spatial non-uniformities of the flip angles (FAs) that are proportional to the B1+ magnitude and result in subject-dependent nonlinear signal inhomogeneities. Thus, accurate B1+/FA mapping methods are needed, particularly for quantitative techniques that require signal intensity corrections[3,4] and parallel RF transmission techniques that require information regarding the B1+ distribution.[5,6]

Various B1+/FA mapping methods have been proposed and can be classified as magnitude-based[7–9] or phase-based.[10,11] In ultrahigh fields, the magnitude methods are considered more applicable mainly because of the robustness to phase shift caused by respiration-induced B0 fluctuations, which can generate substantial errors in phase-based methods.[12,13] Among the former, actual flip angle imaging (AFI), which consists of source images with two types of TRs, can produce relatively low specific absorption rate and can rapidly and accurately measure the distribution of FAs in entire brain areas, particularly when using the utmost nominal (prescribed) FA values, that is, the values set at scanner.[8] However, in our experience, the AFI method sometimes causes substantial underestimations of FAs at 7 tesla (T), suggesting that an appropriate setting of the nominal FA is crucial for accurate FA mapping when using this method. Nevertheless, the setting appears difficult at 7T because the FA distribution in the images exhibits a significant variation mainly due to substantial B1+ heterogeneity[1,2] and there is no practical method to detect the FA calculation errors in the AFI method.

In this study, we implemented computer simulations to elucidate the relationships between FA calculation errors, longitudinal magnetization (Mz), and phase information in the AFI method. Furthermore, we attempted to establish a method using the phase information to detect those errors and optimize the nominal FA values used for human brains at 7T.

Materials and Methods

Computer simulations

We simulated two types of AFI-Mz (Mz_1 and Mz_2) and signals (S_1 and S_2) using the Bloch equation in MATLAB 9.0

[1]Division of Ultrahigh Field MRI, Institute for Biomedical Sciences, Iwate Medical University, Shiwa-gun, Iwate, Japan
[2]MR Applications and Workflow, GE Healthcare Japan Corporation, Hino, Tokyo, Japan

*Corresponding author: Division of Ultrahigh Field MRI, Institute for Biomedical Sciences, Iwate Medical University, 1-1-1, Idaidori, Yahabacho, Shiwa-gun, Iwate 028-3694, Japan. Phone: +81-19-651-5111 (5372), Fax: +81-19-908-8021, E-mail: tsuyoshi@iwate-med.ac.jp

Received: April 15, 2022 | Accepted: September 25, 2022

(MathWorks, Natick, MA, USA). The signals consisted of an interleaved steady-state spoiled gradient echo (SPGR) sequence[14] with two different TRs (TR_1 « TR_2)[10] and true FA values ranging between 1° and 180° (at 0.1° intervals) after 100 excitations with non-selective rectangular RF pulses of 1.0 ms. Transverse magnetization (Mxy) was eliminated by linearly incrementing the phase of consecutive RF excitation pulses with 117°.[14] The following simulation parameters were used: TR_1, 7.1 ms; TR_2, 100 ms; TE, 2.23 ms; longitudinal relaxation time (T1)/transverse relaxation time (T2), 500/70, 1591/90, and 4425/2000 ms (for fat,[15] brain tissue,[16] and water,[17] respectively). Then, we calculated the FAs from both the magnitude signals and the complex signals using a simple approximation by Yarnykh[8] based on the ratio of S_1 and S_2, and the ratio of the TRs, as shown in equation (1).

$$\mathrm{FA} = \arccos([r \times n - 1]/[n - r]) \qquad (1)$$

$$r = S_2/S_1, n = \mathrm{TR}_2/\mathrm{TR}_1$$

Mz_1, Mz_2, and the absolute values of the phase difference between S_1 and S_2 were also calculated. Furthermore, by comparing these values, we examined the relationships between the Mz polarity, phase difference, and errors in the FA calculation.

Phantom experiment and volunteer scan

We used a 7T MRI scanner (Discovery MR950; GE Healthcare, Waukesha, WI, USA) with a 2-channel transmit and 32-channel receive head coil system (NM008-32-7GE-MR950; Nova Medical, Wilmington, MA, USA). All scans were performed with RF transmissions of a circular polarization mode.

We performed 3D AFI scans of a 16 cm-diameter sphere phantom that contained 2.5%wt saline-based agarose gel with a T1 value of 1519.0 ms (standard deviation, 29.9 ms), setting the nominal FA to values from 5° to 130° in 5° intervals. The scanning parameters used were as follows: sequence, SPGR; excitation RF pulse, non-selective rectangular pulse of 1.0 ms; TR_1/TR_2, 7.1/100.0 ms; TE, 2.23 ms; FOV, 22.0 × 22.0 cm; scan matrix, 96 × 96 × 44; voxel size, 2.3 × 2.3 × 8.0 mm^3 (interpolated to 1.7 × 1.7 × 4.0 mm^3 after zero-filled Fourier transformation); bandwidth, 390.6 Hz/pixel; average, 1; and acquisition time, 7 min 6s. Real, imaginary, and magnitude images were obtained.

In addition, to obtain the reference FA values, we performed time-consuming 3D variable FA (VFA) scans[7] using nominal FA values of 5.0°, 10.6°, 16.2°, 21.9°, 27.5°, 33.1°, 38.8°, 44.4°, 50.0°, 60.0°, 70.0°, 80.0°, and 90.0°, which has been reported as an accurate FA measurement method to 180° because of the usage of multiple data with various nominal FAs and T1 map data.[18] The following scanning parameters were also used: sequence, SPGR; excitation RF pulse, non-selective rectangular pulse of 1.0 ms; TR, 100 ms; TE, 2.23 ms; FOV, 22.0 × 22.0 cm; scan matrix, 96 × 32 × 44; voxel size, 2.3 × 6.9 × 8.0 mm^3 (interpolated to 1.7 × 1.7 × 4.0 mm^3); bandwidth, 390.6 Hz/pixel; average, 1; and acquisition time, 23 min 15 s. The T1 map of the phantom was also calculated using an inversion recovery method with inversion times of 20, 50, 80, 155, 312.5, 625, 1250, 2500, 5000, and 10000 ms. The FA values were then obtained by fitting the 3D VFA and T1 data to a known SPGR signal model[14] using the nonlinear least-squares method.

Finally, five healthy subjects with no neurological signs or symptoms were recruited for the volunteer scans (four men and one woman; age range, 37–59 years; median, 44 years). All procedures were approved by the Institutional Ethics Committee (H25-53) and written informed consent was obtained from all participants. We performed AFI scans of their heads with nominal FA values between 10° and 90° at 10° intervals. The remaining scan parameters were the same as those used in the phantom tests.

Image analyses

Using an in-house program, we generated FA maps of the phantom based on the data obtained from both the magnitude-based AFI and VFA methods. In addition, we calculated the phase and absolute values of the phase difference between S_1 and S_2 of the AFI and used the results to generate the phase-difference maps. We then analyzed the relationships between signal intensity, phase difference, FA values from the AFI method, and FA values from the VFA method within a 15 cm-diameter spherical ROI centered on the phantom. A linear regression analysis was performed to examine the correlation between the FA values obtained from the AFI and VFA methods for cases where the corresponding phase difference was below the threshold value determined through the simulation. The phase difference was curve-fitted using a sigmoid function that approximated a step function to confirm the validity of the threshold. In addition, using this threshold value for the phase difference, we generated error maps that indicated pixels with erroneous FA values. Pixels with S_1 or S_2 within the noise level[19] or resulting out-of-range values for Equation (1) were designated as unmeasurable FA values.

Similarly, we generated FA maps from the AFI images of the volunteers' heads and obtained error maps using the phase difference threshold. To analyze the ratio between the areas with appropriately or inappropriately measured FAs and that of the whole-brain FA mapping, the brain tissue region was extracted from the TR_2 AFI source images using the extraction tool[20] of the FMRIB software library[21] with a brain extraction threshold of 0.77. The image uniformity of the TR_2 source images was corrected before brain extraction using the intensity nonuniformity correction algorithm implemented in SPM12 (the Functional Imaging Laboratory, the Wellcome Trust Centre for Neuroimaging, the Institute of Neurology, University College London, UK).

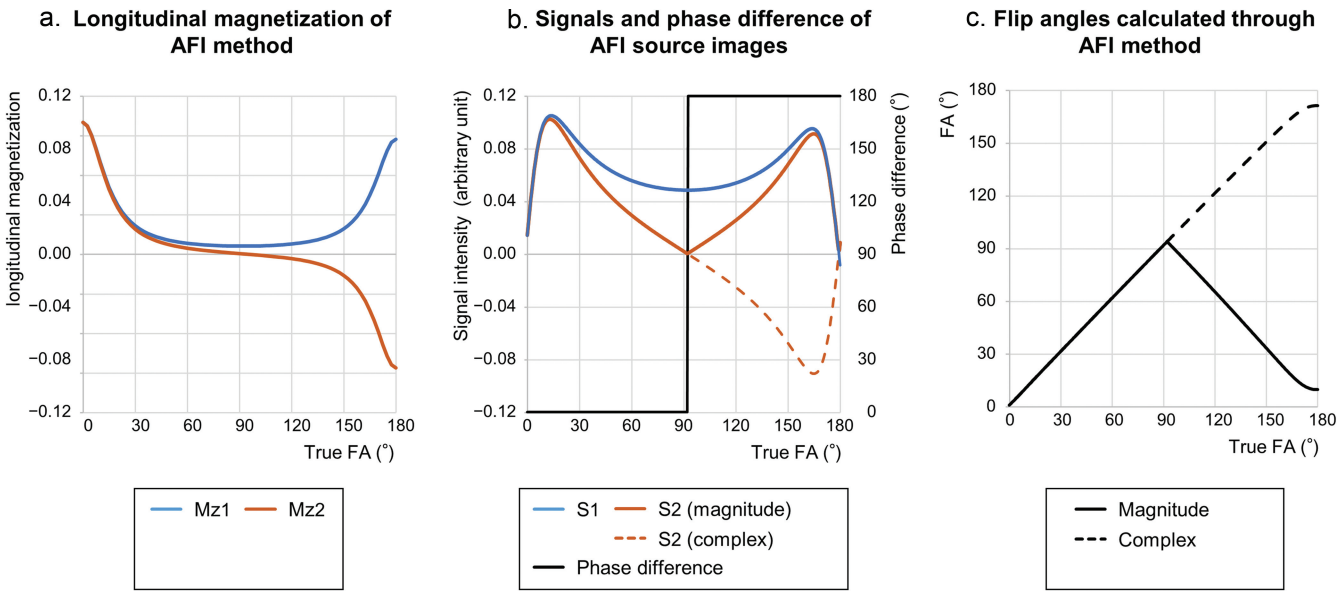

Fig. 1 Computer simulation of longitudinal Mz, SI, phase difference, and FA in the AFI method. **a**: When the true FA exceeds 93°, Mz_2 is inverted (red line) but Mz_1 is not inverted (blue line), resulting in MZ_1 and MZ_2 in the opposite direction. **b**: SI for S2, one of the source signals, turns negative under the complex condition (dashed red line) and is symmetrically increased under the magnitude condition (solid red line) when the true FA exceeds 93°, at which the phase difference increases from 0° to 180° (black line), whereas SI for S1 remains positive (blue line). **c**: Under the magnitude condition, the calculated FA values are incorrect beyond a true FA of 93° (solid black line). AFI, actual flip angle; FA, flip angle; Mz, magnetization; SI, signal intensity.

Results

The computer simulation revealed that the interleaved scan with two identical RFs of different TRs induced non-inversion of the Mz_1 polarity and inversion of the Mz_2 polarity for a true FA of approximately 93° (Fig. 1a), for which the phase difference between S_1 and S_2 leaped from 0° to 180° because of the opposite polarity between Mz_1 and Mz_2 (Fig. 1b, black line). Furthermore, beyond this point, while S_1 remained positive, S_2 continued to decrease to negative values under a complex condition and showed symmetrically positive values under a magnitude condition (Fig. 1b, red lines). Consequently, the FA values calculated by the AFI method showed erroneous values beyond the true FA of 93° (Fig. 1c, solid line). The true FAs that showed this phenomenon were almost identical for all three T1/T2 combinations (92.5°–92.7°). Based on the results, we defined the mean between 0° and 180°, that is, 90°, as the threshold of the phase difference that predicts FA calculation errors in scans of the phantoms and human brains.

In the tests with the phantom, when compared with S_1 signals, the intensity of S_2 signals, as a function of FAs computed using the VFA method, remarkably decreased for FAs of up to 90° and then increased with augmented variances, confirming the characteristics of the AFI signals that were observed in the simulation (Fig. 2a). In addition, the phase differences between S_1 and S_2 dramatically increased beyond VFA-based FA values of approximately 90° (Fig. 2a) and were well fitted by the sigmoid function $y = 171.2/\{1+\exp(-0.05 \times [x - 98.42])\}$ (Fig. 2b), which reflected the non-inverted and inverted polarities of Mz_1 and Mz_2, respectively, as indicated in the simulation. Furthermore, the FAs computed using the AFI method and corresponding to phase differences under the threshold of 90° showed excellent positive correlation and agreement with those computed using the VFA method (Pearson correlation coefficient, $r = 0.98$ [$P < 0.001$], $y = 0.87x + 1.94$; intraclass correlation coefficients = 0.99 [95% confidence interval, 0.99%–0.99%]) (Fig. 2b).

In the FA maps of the phantom, the FA distribution obtained using the AFI method was considerably different from that obtained using the VFA method. On the error maps generated by applying 90° as the threshold of the phase difference, only a small area of erroneous FAs was found at the center of the image with a nominal FA of 50°, which expanded as the nominal FA increased from 70° to 80° (Fig. 3). These findings appear to correspond to the phase inversion of the S2 phase maps. In contrast, substantial areas of unmeasurable FAs were observed in the peripheral areas when the nominal FAs were 30° and 50° (Fig. 3).

The tests on volunteer subjects demonstrated that errors in the FA calculation using the AFI method were visually evident in both the FA and error maps when the nominal FAs exceeded 60°, and the error areas were comparable to those with phase inversion in the S2 phase maps (Fig. 4). The area fraction of the whole brain with appropriate FA values was the highest for nominal FAs of 40°–60° {median, 0.996–0.998 (interquartile range [IQR], 0.001–0.004)}, coinciding

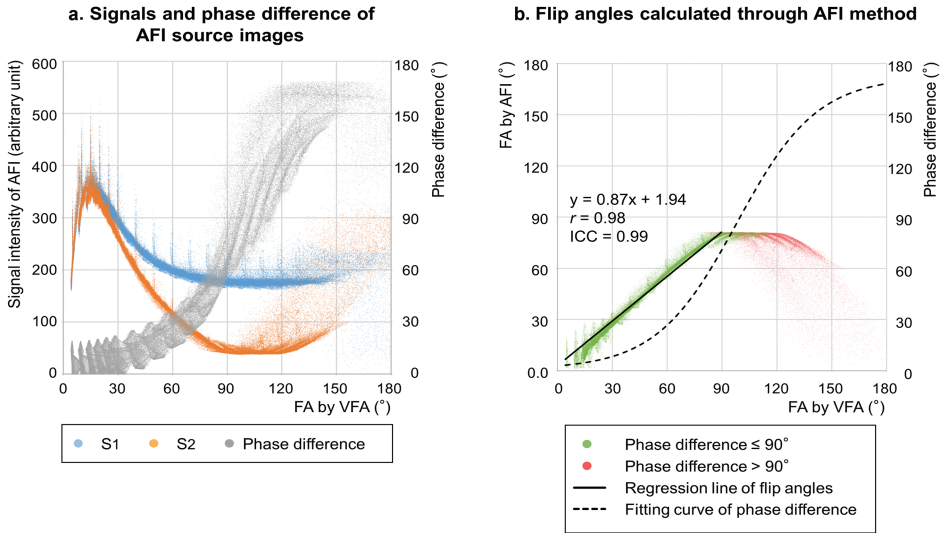

Fig. 2 SI, phase difference, and FA of the phantom in the AFI method. **a**: The SI distributions for S_1 (blue dots) and S_2 (red dots), as well as the phase difference between them (gray dots), are generally comparable to those in the simulation. **b**: FA values obtained using the AFI method with phase differences ≤90° (green dots) show excellent positive correlation and agreement with those obtained using the VFA method. Dotted line: fitting curve of the phase difference. AFI, actual flip angle; FA, flip angle; SI, signal intensity; VFA, variable flip angle.

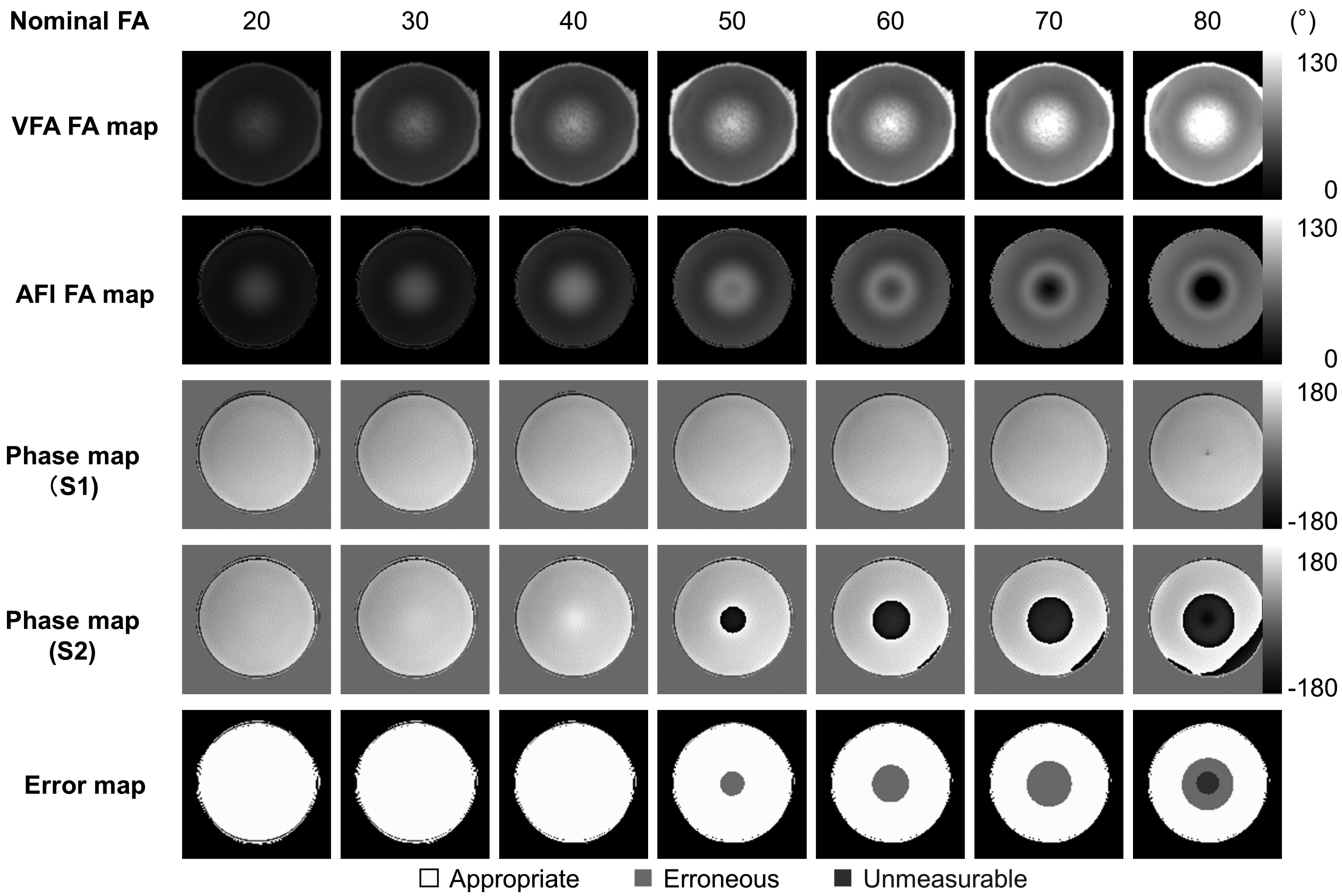

Fig. 3 FA, phase, and error maps of the phantom using the AFI method and FA maps of the VFA method. The FA maps calculated using the AFI method are considerably different from those calculated using the VFA method for nominal FAs of 70° or higher, whereas these maps are comparable for FAs of 50° or lower. Phase opposition is evident only in the S2 phase maps. The error maps generated from the phase-difference information readily identify pixels with inappropriate FA values as either erroneous or unmeasurable. AFI, actual flip angle; FA, flip angle; VFA, variable flip angle.

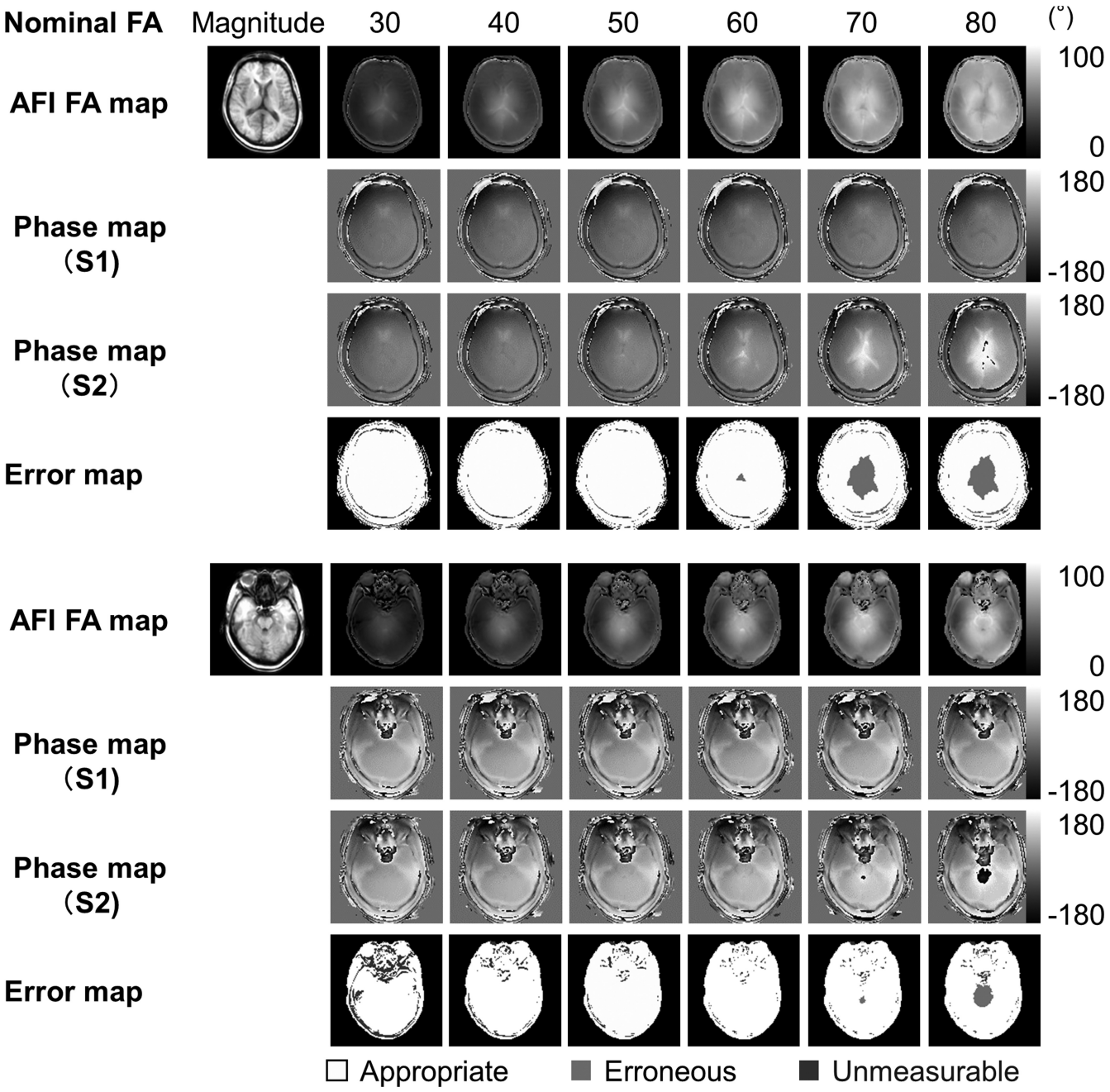

Fig. 4 FA, phase, and error maps of a human head in the AFI method. A 59-year-old healthy man. The phase maps show apparent phase differences between S1 and S2 for nominal FAs ≥ 60°. The error maps clearly indicate the pixels with incorrect FA values, mainly due to insensitivity to the Mz polarity, on the images with nominal FAs of 60°, 70°, and 80°. AFI, actual flip angle; FA, flip angle; Mz, magnetization.

with minimal areas of erroneous or unmeasurable FA (Fig. 5). In contrast, the area fractions of erroneous FAs substantially increased for nominal FAs of 70°, 80°, and 90° (0.008 [0.004], 0.028 [0.008], and 0.162 [0.032], respectively), whereas those of unmeasurable FAs increased for nominal FAs of 30°, 20°, and 10° (0.034 [0.019], 0.100 [0.042], and 0.232 [0.078], respectively) (Fig. 5). These results suggest that nominal FAs of 40°–60° are appropriate to calculate FAs in the entire brain using the AFI method in the 7T system that we used.

Discussion

In this study, using the phase difference information between the S_1 and S_2 source images, we successfully detected pixels showing erroneous FAs owing to insensitivity to the Mz

polarity on the magnitude images used in FA mapping derived from the AFI method. In addition, by applying this method to human brains at 7T, we found that nominal FA values greater than 60° are unsuitable and values between 40° and 60° should be selected for accurate FA measurements in the system that we used. To our knowledge, this is the first report to introduce a practical method for determining calculation errors in FA values using the AFI method and estimating the appropriate nominal FAs in AFI scans.

The simulation in this study demonstrated the characteristic spin behavior of the AFI method. When the FA exceeds 90°, consecutive interleaved excitations with two different TRs induce a steady-state condition of Mz_1 and Mz_2 with opposite polarities, that is, non-inverted Mz_1 and inverted Mz_2, which is a cardinal cause of the FA calculation errors. In addition, the opposite polarities of Mz_1 and Mz_2 result in a phase opposition between S1 and S_2. The inversion of Mz_2 at 93°, but not at 90°, in the simulation can be explained by the longitudinal relaxation of Mz_2 during TR.

This study demonstrated that the results of the phantom tests were generally comparable to those of the computer simulation. However, we found substantial variances in signal intensity and phase difference of the source images, as well as in values of the FAs calculated using the AFI method, particularly when the FA values obtained via the VFA method exceeded 90°. This issue can be mainly attributed to the fact that close to a VFA-FA of 90°, the signal intensity of S_2 diminishes below the noise level, which depends on the sensitivity distribution of the receiving coils. Inhomogeneity of the intravoxel FA distribution can also cause continuous phase difference distribution, which ranges from 0° to 180°. In addition, the phase difference and flip angle varied or were unmeasurable below a VFA-FA of 30°, because the difference in signal intensity between the S_1 and S_2 images was minimized. Therefore, further improvement of the SNR can solve these issues to some extent, as pointed out in a previous study.[8]

In the phantom experiment, we used the VFA method as the reference for calculating FA values because this method has been reported to enable the measurement of FAs with high accuracy owing to the use of multiple data with various nominal FAs and T1 data.[18] However, the VFA method can inherently include non-negligible errors, particularly in ultra-high fields. Variations in the FA distribution due to spatial B1+ inhomogeneity at 7T can affect the FA values calculated through the nonlinear least-squares regression used in the VFA method. Further optimization of the TR or the nonlinear calculation algorithm used in the VFA method may improve the accuracy of FA measurements, although this issue is beyond the scope of this study.

The FA calculation errors in the AFI method are mainly caused by the use of the magnitude images, which are insensitive to the Mz polarity, as source images. When Mz_1 and Mz_2 are opposite, calculations using the magnitude signals of S_1 and S_2 yield errors in the FA values. This phenomenon is independent of the magnetic field strength, but is more likely

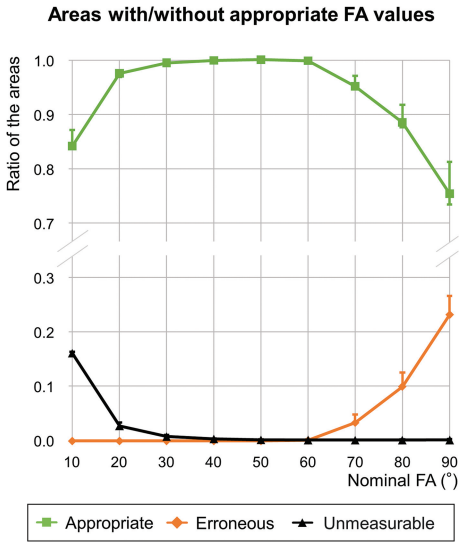

Fig. 5 Areas with appropriate/inappropriate FA values of the human heads in the AFI method. The areas with appropriate FA values (green line) in the whole brains of five volunteers reached nearly 100% for nominal FAs of 40°–60°, whereas those with erroneous FA (orange line) and unmeasurable (black line) FA values were substantial for nominal FAs ≥ 70° and ≤ 30°, respectively. AFI, actual flip angle; FA, flip angle.

to occur at 7T because of the profound inhomogeneity of the B1+ distribution. The extended version of the AFI method incorporating Mz polarity to correct FA values[22] or phase-sensitive imaging techniques that include information regarding the Mz polarity can be a solution to avoid this issue. However, in the extended AFI method, substantial calculation errors can occur due to polarity changes of background noise. In the phase-sensitive imaging method, estimation of the background phase information as well as accurate phase correction in terms of background phase variation and initial phase component appear challenging, particularly under augmented B1+ heterogeneity at 7T.[23,24] In contrast, the detection of the error pixels in terms of FA calculation using phase information, which we used, is considered a robust and easy-to-use solution because Mxy can be cancelled by subtraction in the calculation process and the incorrect FA values can be determined only by the Mz polarity for various subjects, body locations, and scanners.

The parameter settings for the AFI scans in this study were not identical to those used in previous studies. For accurate measurements of the FAs in various tissues with heterogeneous T1 values, we used the shortest TR_1 to minimize the spin relaxation of Mz_2. This setting resulted in a TR_2/TR_1 ratio of 14.1, which is substantially larger than 4–6, which was proposed to maintain the SNR in a previous study.[8] This setting is considered to contribute to the fact that the areas with unmeasurable FA were minimal on the volunteer images, although the reduced SNR may have affected the accuracy of the FA measurement to some extent.

In addition to the AFI method, several magnitude-based methods have been proposed for B1+/FA mapping, such as the double angle method[8] and the dual refocusing echo acquisition mode method.[11] In these methods, as in the AFI method, an appropriate setting of the nominal FA is crucial to diminish the calculation errors, particularly at 7T. The technique using phase difference information, which we introduced, can be applicable to these magnitude-based methods as well and may be helpful to improve the accuracy of measurements.

This study has several limitations. First, the appropriate nominal FAs that we found, which strongly depend on the static magnetic field, RF transmission system, and body location, cannot be generalized to those for other scanners. The nominal FAs for the AFI method should be optimized for each scanner system, body location, and maybe for each subject when intersubject differences are substantial. Second, we did not perform validation studies using the other 7T systems. Therefore, it remains unclear whether the method using phase-difference information can be applied to other scanners or vendors. It also remains unknown whether the proposed method is still effective at a lower magnetic field, e.g. 3T, which yields lower SNRs. Third, this study did not include patients with neurological disorders such as cerebrovascular diseases, brain tumors, demyelinating diseases, and degenerative disorders. Thus, we cannot determine whether the detection of the FA-calculation errors using phase information can contribute to accurate measurement of FAs in pathological tissues, although the simulation study indicated that differences in T1 and T2 do not significantly contribute to the accuracy of the detection. Fourth, we used the TR_2 value introduced in the original study without any optimization, although the SNR and phase information can be altered by setting TR_2. Further optimization of the TR_2 value may improve the accuracy of FA detection. Another technical limitation is that we adopted full-echo sampling for the AFI method to obtain phase information, which resulted in prolongation of the TE (2.23 ms) when compared with the minimum TE (1.45 ms) using a partial echo technique. This might have slightly affected the accuracy of the AFI method used in this study.

Conclusion

The phase difference between the two types of AFI source images can be used to detect pixels with erroneously calculated FA values owing to their insensitivity to the Mz polarity. This method helps determine the appropriate nominal FAs to be used in the AFI method to accurately measure FA distribution.

Funding

This study was partly supported by JSPS KAKENHI (18H00483).

Conflicts of Interest

Yuji Iwadate is an employee of GE Healthcare Japan Corporation. The other authors have no conflicts of interest.

References

1. Hoult DI, Phil D. Sensitivity and power deposition in a high-field imaging experiment. J Magn Reson Imaging 2000; 12:46–67.
2. Collins CM, Liu W, Schreiber W, Yang QX, Smith MB. Central brightening due to constructive interference with, without, and despite dielectric resonance. J Magn Reson Imaging 2005; 21:192–196.
3. Windschuh J, Zaiss M, Meissner JE, et al. Correction of B1-inhomogeneities for relaxation-compensated CEST imaging at 7T. NMR Biomed 2015; 28:529–537.
4. Oz G, Deelchand DK, Wijnen JP, et al. Advanced single voxel ^{1}H magnetic resonance spectroscopy techniques in humans: experts' consensus recommendations. NMR Biomed 2020 Jan 10:e4236. [Epub ahead of print]
5. Katscher U, Bornert P, Leussler C, van den Brink JS. Transmit SENSE. Magn Reson Med 2003; 49:144–150.
6. Zhu Y. Parallel excitation with an array of transmit coils. Magn Reson Med 2004; 51:775–784.
7. Venkatesan R, Lin W, Haacke EM. Accurate determination of spin-density and T_1 in the presence of RF-field inhomogeneities and flip-angle miscalibration. Magn Reson Med 1998; 40:592–602.
8. Yarnykh VL. Actual flip-angle imaging in the pulsed steady state: a method for rapid three-dimensional mapping of the transmitted radiofrequency field. Magn Reson Med 2007; 57:192–200.
9. Nehrke K, Bornert P. DREAM—a novel approach for robust, ultrafast, multislice B_1 mapping. Magn Reson Med 2012; 68:1517–1526.
10. Morrell GR. A phase-sensitive method of flip angle mapping. Magn Reson Med 2008; 60:889–894.
11. Sacolick LI, Wiesinger F, Hancu I, Vogel MW. B_1 mapping by Bloch-Siegert shift. Magn Reson Med 2010; 63:1315–1322.
12. Van de Moortele PF, Pfeuffer J, Glover GH, Ugurbil K, Hu X. Respiration-induced B_0 fluctuations and their spatial distribution in the human brain at 7 Tesla. Magn Reson Med 2002; 47:888–895.
13. Harada T, Kudo K, Uwano I, et al. Breath-holding during the calibration scan improves the reproducibility of parallel transmission at 7T for human brain. Magn Reson Med Sci 2017; 16:23–31.
14. Zur Y, Wood ML, Neuringer LJ. Spoiling of transverse magnetization in steady-state sequences. Magn Reson Med 1991; 21:251–263.
15. Bojorquez JZ, Bricq S, Acquitter C, Brunotte F, Walker PM, Lalande A. What are normal relaxation times of tissues at 3T? Magn Reson Imaging 2017; 35:69–80.
16. Marques JP, Kober T, Krueger G, van der Zwaag W, Van de Moortele PF, Gruetter R. MP2RAGE, a self bias-field corrected sequence for improved segmentation and T1-mapping at high field. Neuroimage 2010; 49:1271–1281.
17. Daoust A, Dodd S, Nair G, et al. Transverse relaxation of cerebrospinal fluid depends on glucose concentration. Magn Reson Imaging 2017; 44:72–81.

18. van Schie JJ, Lavini C, van Vliet LJ, Vos FM. Feasibility of a fast method for B_1-inhomogeneity correction for FSPGR sequences. Magn Reson Imaging 2015; 33:312–318.
19. Otsu N. A threshold selection method from gray-level histograms. IEEE Trans Syst Man Cybern 1979; 9:62–66.
20. Smith SM. Fast robust automated brain extraction. Hum Brain Mapp 2002; 17:143–155.
21. Woolrich MW, Jbabdi S, Patenaude B, et al. Bayesian analysis of neuroimaging data in FSL. Neuroimage 2009; 45(Suppl): S173–S186.
22. Morrell GR, Schabel MC. An analysis of the accuracy of magnetic resonance flip angle measurement methods. Phys Med Biol 2010; 55:6157–6174.
23. Kellman P, Arai AE, McVeigh ER, Aletras AH. Phase-sensitive inversion recovery for detecting myocardial infarction using gadolinium-delayed hyperenhancement. Magn Reson Med 2002; 47:372–383.
24. Wang J, Chen H, Maki JH, et al. Referenceless acquisition of phase-sensitive inversion-recovery with decisive reconstruction (RAPID) imaging. Magn Reson Med 2014; 72:806–815.